Int. J. Heat Mass Transfer. Vol. 34, No. 12, pp. 3097–3106, 1991
Printed in Great Britain

0017–9310/91 $3.00 + 0.00

Analysis of close-contact melting for octadecane and ice inside isothermally heated horizontal rectangular capsule

T. HIRATA and Y. MAKINO
Department of Mechanical Systems Engineering, Shinshu University, 500 Wakasato, Nagano 380, Japan

and

Y. KANEKO
Takasago Thermal Engineering Co., Ltd, 4-2-8 Kanda Surugadai, Chiyoda-ku, Tokyo 101, Japan

(*Received* 6 *November* 1990 *and in final form* 25 *January* 1991)

Abstract—Close-contact melting characteristics of phase change materials (PCM) inside horizontal rectangular capsules are examined experimentally. The capsules are heated isothermally and three kinds of aspect ratios ($H/W = 3$, 1 and 1/3) are provided. Octadecane and ice are used, respectively, as PCM. A method of analysis applying Nusselt's liquid film theory to the close-contact melting heat transfer in the rectangular capsule is presented. The analytical results show good agreement with the experimental data. For the melting of ice, it is found that the effect of natural convection resulting from density inversion of water at 4°C becomes significant for large Stefan numbers.

INTRODUCTION

MELTING or solidification of PCM is of great interest in engineering applications such as thermal energy storage systems. The latent heat of phase change has become widely utilized, for example, for the effective utilization of solar energy and for the latent heat storage of a heat-pump air conditioning system.

In recent years, a compact heat exchanger combined with thermal storage capsules has been developed. With regard to that heat exchanger, close-contact melting on a plate-fin [1, 2] and phase change characteristics of a PCM-built-in heat exchanger [3] have been studied. In those applications, the heat transfer as well as phase change phenomena of PCM are different from those inside a cylindrical capsule. With regard to the melting phenomena inside a cylindrical capsule, two kinds of melting patterns are observed depending on heat conditions at both ends of the capsule. One is that the solid is fixed and the melting is controlled mainly by natural convection heat transfer, and the other is that the solid is unfixed and close-contact melting dominates. It is, therefore, important to establish the melting phenomena for the above two patterns.

For the close-contact melting problem, Saito *et al.* [4, 5] examined the effect of ablation at the solid–liquid interface by numerical analysis. Moallemi *et al.* [6] obtained an analytical solution taking into consideration transport of sensible heat in the close-contact melting layer. In the present study the experiments were performed for close-contact melting inside isothermally heated horizontal rectangular capsules. Octadecane and ice were used as PCM, respectively, and three kinds of aspect ratios were chosen for the rectangular capsules. Analytical results were also obtained by applying Nusselt's liquid film theory to heat transfer in the close-contact liquid layer. The melting phenomena, the thickness of the melt layer, and also the effect of natural convection in the liquid phase on the melting process are discussed.

EXPERIMENTAL APPARATUS AND PROCEDURE

The experimental apparatus consisted of a test section, a constant temperature water bath (or ethylene glycol solution) and a recirculating system of the fluid. The test capsule consisted of a 100 mm long rectangular copper tube, of 50.7×50.7 mm or 30.8×90.4 mm cross-sectional area, having a wall thickness of 2.0 mm. The test capsule, filled with n-octadecane (99% pure) or water, was closed at both ends by transparent acrylic resin plates, so that the melting process could be observed. The volumetric change associated with phase change from solid to liquid was accommodated by an overflow outlet at one end of the capsule. Heating of the test capsule was carried out by showering hot water from the constant temperature bath with high velocity around the copper wall of the capsule. Prior to the melting experiment, the test capsule was immersed in an auxiliary constant-temperature bath, the temperature of which was 1.5–2.0°C lower than the melting temperature of the PCM. After a steady-state condition

NOMENCLATURE

$A(\tau)$	dimensionless molten mass fraction
B	aspect ratio of capsule, H/W
C	equation (22)
C_{p_l}	specific heat of liquid
Fo	Fourier number, $\kappa_l t/W^2$
g	gravitational acceleration
h	heat transfer coefficient
H	height of capsule
L	latent heat of fusion
m	molten mass fraction per unit area and unit time
Nu_w	Nusselt number, hW/λ_l
p	pressure
Pr	Prandtl number, ν/κ
q	heat flux
s	molten mass fraction, s_l+s_δ
s_l, s_δ	molten mass fractions at bottom and top of capsule
s_c	critical thickness of liquid phase, equation (24)
Ste	Stefan number, $C_{p_l}(T_w-T_f)/L$
t	time
T	temperature
T_f, T_w	melting and wall temperatures
u	velocity in the x-direction
W	width of capsule
x, y	coordinates.

Greek symbols

δ	thickness of liquid layer
κ_l	thermal diffusivity of liquid
λ_l	thermal conductivity of liquid
μ_l	dynamic viscosity of liquid
ν_l	kinematic viscosity of liquid
ρ_l, ρ_s	densities of liquid and solid
τ	dimensionless time, $Ste\ Fo$.

Superscript

*	dimensionless values, equation (14).

was reached, the test capsule was set up in the test section for the melting experiment. Through the experiment, the capsule wall temperatures, T_w, measured at the top and bottom, respectively, showed a difference of about 5% of (T_w-T_f). Since close-contact melting is the main object in the present study, the temperature where the solid contacts with the capsule wall was chosen as a value of T_w.

For the ice melting experiment, if a small amount of air bubbles are involved in the test ice, the heat transfer characteristics at the close-contact area will be affected by the bubbles accumulating in the close-contact liquid layer. In the preparatory experiments, it was observed that this effect was much more significant for the ice experiment than for the octadecane. For the ice experiment, close-contact melting occurs at the top of the capsule and the air bubbles stagnate in the liquid layer, while for the octadecane, the close-contact occurs at the bottom and the air bubbles are easily removed by the flow in the liquid layer. Therefore, for the ice experiment, an ice block, from which the test ice containing no air bubble was obtained, was made in a large vessel of 5000 cm^3 vol.; a completely transparent portion was cut out from the ice block and was packed in the test capsule.

During the melting experiments, the solid–liquid interface was photographed at predetermined time intervals to measure the molten mass fraction. Solid and liquid regions on the photographic paper were cut out, respectively, and the molten mass fraction was evaluated by measuring the weight of both the solid and liquid pieces with a precision balance. The error of this device was estimated to be within $\pm 2.5\%$ for the molten mass fraction. Two-dimensionality of heat flow from the capsule wall to the solid–liquid interface was ascertained by the fact that the melting shape of the PCM showed almost two-dimensionality. The aspect ratios of the test capsules used were $H/W(=B) = 1/3$, 1 and 3, respectively, where H is capsule height and W is capsule width. The melting temperature of octadecane was estimated from the experiments as $T_f = 27.8°C$. The experimental ranges covered in the present experiments were $(T_w-T_f) = 2.2$–$20.2°C$. The symbols for each experimental condition are shown in Table 1.

MELTING PHENOMENA

Figures 1(a)–(c) show typical results of melting phenomena of octadecane for aspect ratios of $B = 1/3$, 1 and 3, respectively. In Figs. 1(a) and (b), close-contact melting is observed at the bottom of the capsule and the melting proceeds, keeping the solid at a level. It is shown that the melting occurs also from the side walls by heat conduction, however, the effect of natural convection at the side walls on melting can be regarded as negligible judging from the solid shape of the upper corners. The liquid at the upper region of the capsule is stable since the temperature of the capsule wall is higher than the melting temperature. Therefore, the melting at the top surface of the solid is dominated by heat conduction from the top wall through the stable liquid.

In Fig. 1(c) for the larger aspect ratio, it is shown that the solid inclines to either of the side walls and is in contact with it. In this case, it was observed that the solid rotated through about 90° during the melting process, since close-contact melting occurred also at

Table 1. Experimental conditions and symbols

$B = 1/3$			$B = 1$			$B = 3$		
Symbol	ΔT (°C)	*Ste*	Symbol	ΔT (°C)	*Ste*	Symbol	ΔT (°C)	*Ste*
				n-Octadecane				
●	2.6	0.0287	■	2.2	0.0243	▲	2.2	0.0243
◑	6.7	0.0739	◪	7.1	0.0784	◭	7.3	0.0806
◓	11.4	0.126	◥	12.4	0.137	◭	12.0	0.132
◒	19.6	0.216	◥	19.6	0.216	◬	20.2	0.223
				Ice				
○	2.9	0.0365	□	2.8	0.0354	△	2.9	0.0365
⊙	8.0	0.101	⊡	8.1	0.102	◬	8.0	0.101
◍	13.0	0.163	◪	13.0	0.163	◬	12.7	0.159
⊖	20.0	0.251	◹	20.0	0.250	◬	19.8	0.248

the side wall. At this stage of the present study, it is difficult to predict the aspect ratio of the onset conditions whether the solid inclines or not. It can be noted, however, that the solid does not incline at least for $B \leqslant 1$.

For the melting of ice, the melting phenomena for $T_w < 4°C$ are the same as those results shown in Figs. 1(a)–(c) inverted. On the other hand, for $T_w > 4°C$, the water at the bottom of the capsule is unstable and natural convection occurs when the Rayleigh number exceeds the onset value. In this case, the melting at the under-surface of the ice is dominated by natural convection heat transfer as observed in Fig. 1(d).

Figures 2 and 3 show dimensionless molten mass fraction during the transient melting process for octadecane and ice, respectively. In Fig. 2, it is shown that the melting rate for $B = 1/3$ is faster than that for $B = 1$ at all the temperature conditions. If it is supposed that the melting occurs in the two same capsules of $B = 1/3$ and 1, respectively, the gravitational force acting on the solid per unit of close-contact area is larger for $B = 1$, since the close-contact area is smaller for $B = 1$. Figure 2 implies that the close-contact area is much more dominant than the gravitational force for the melting rate. This is also verified by the results for $B = 3$, showing a faster melting rate than those for $B = 1$, due to inclination of the solid causing large close-contact area as observed in Fig. 1(c). From the above discussions, in order to produce a faster melting rate, the aspect ratio of the capsule should be taken as $B < 1$ or $B > 1$.

Comparison between Figs. 2 and 3 reveals that the melting of ice is twice as fast as octadecane, although the latent heat of ice (335 kJ kg^{-1}) is larger than that of octadecane (241 kJ kg^{-1}). The difference between their Stefan numbers is 10–20% (Table 1) and is not as large as the difference of the melting time. By reference to the definition of dimensionless time (see equation (14)), it can be seen that the melting rate of ice is faster than that of octadecane because thermal diffusivity of water is larger than that of octadecane.

For the melting of ice shown in Fig. 3, it is seen that the effect of B is apparently small compared with the results for octadecane. This is caused by the difficulty of packing ice into the test capsule. In the present experiment, non-bubble ice was used as the test ice, however, during the process of packing, when the water being inserted between the test ice and the capsule wall was frozen, a small amount of air bubbles always accumulated on the freezing interface and it was impossible to eliminate those bubbles completely. In Fig. 3, it is presumed that the air bubbles affect the melting rates to some degree. For the capsule with a smaller width, the bubbles were easily removed by the flow in the close-contact liquid layer, while for the one with a larger width the bubbles tend to be retained. For a smaller value of B, therefore, the effect of bubbles became significant and the melting rate became slower than that for completely non-bubble ice. For the melting of octadecane, this effect was undetectable.

ANALYSIS USING NUSSELT'S LIQUID FILM THEORY

Melting for octadecane

If it is assumed that (1) the melting proceeds keeping the solid at a level, (2) the melting is dominated by heat transfer in the close-contact layer at the bottom and by heat conduction through the stable liquid at the top, and (3) the melting from the side walls is negligible as compared with the total molten mass fraction, an analytical model for the physical problem is represented by the schematic diagram shown in Fig. 4, where s_δ and s_l are the molten mass fractions by heat conduction from the top wall and heat transfer from the bottom wall, respectively. In the present paper, it is defined that 'liquid phase' denotes the liquid at the top region, and 'liquid layer', denotes the thin liquid layer in the close-contact region at the bottom.

It was reported that the two-dimensional liquid layer shown by the enlarged scale in Fig. 4 is, in general, very thin. For example, Saito *et al.* [4] reported that the thickness of the liquid layer for close-contact melting of circular cross-sectional solid was 0.014–0.16 mm. Therefore, if it is assumed for the liquid layer that: (a) the liquid is Newtonian, (b) the

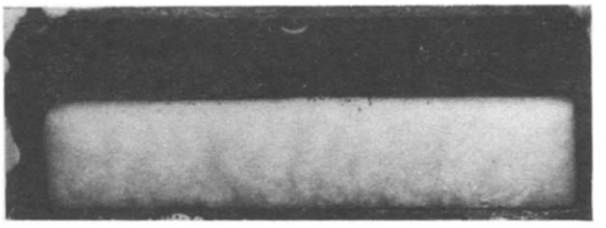

(a)

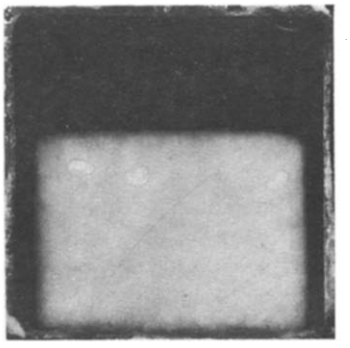

(b)

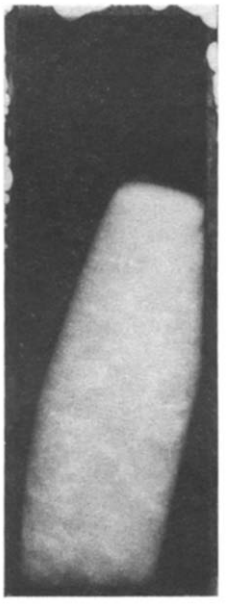

(c)

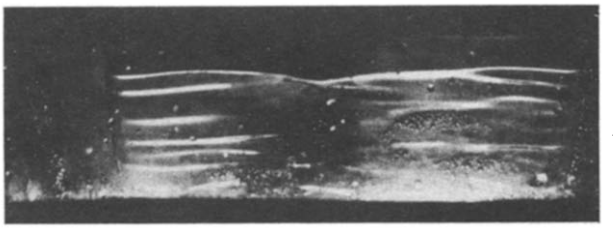

(d)

FIG. 1. Melting phenomena for octadecane (a–c) and ice (d). (a) $B = 1/3$, $\Delta T = 11.4$°C, $t = 360$ s. (b) $B = 1$, $\Delta T = 12.4$°C, $t = 540$ s. (c) $B = 3$, $\Delta T = 12.0$°C, $t = 480$ s. (d) $B = 1/3$, $\Delta T = 20.0$°C, $t = 360$ s (photograph taken from below the capsule).

inertia term of the momentum equation is negligible as compared with the viscous term, (c) heat transport by convective flow is negligible as compared with that by heat conduction, (d) effect of blowing (or suction) at the solid–liquid interface due to volumetric change by melting is negligible, (e) thermo-physical properties are constant values, and (f) flow of the liquid layer is symmetric at $x = 0$; then, the so-called Nusselt liquid film theory is applicable to the melting process. Momentum and energy equations are, therefore, given as follows, respectively:

$$\mu_l \frac{\partial^2 u}{\partial y^2} = \frac{\mathrm{d}p}{\mathrm{d}x} \tag{1}$$

$$\frac{\partial^2 T}{\partial y^2} = 0. \tag{2}$$

The heat balance equation for the region $x = 0 - x$ in

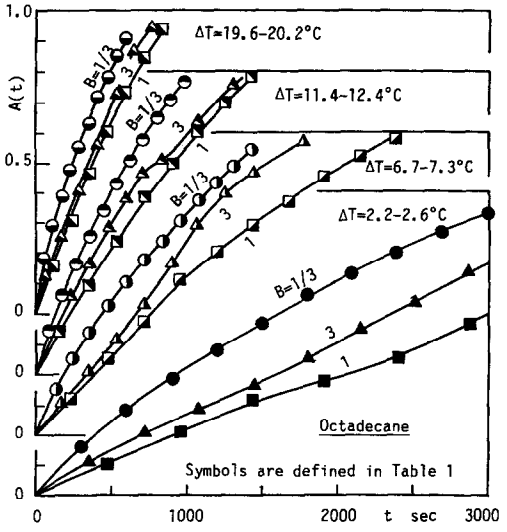

FIG. 2. Molten mass fraction for octadecane.

the liquid layer is given by neglecting a transport of sensible heat ($Ste \ll 1$) as

$$-\int_0^x \lambda_l \left.\frac{\partial T}{\partial y}\right|_{y=0} \mathrm{d}x = \rho_l L \int_0^\delta u \,\mathrm{d}y. \tag{3}$$

The body force acting on the liquid layer is given by

$$2\int_0^{W/2} p \,\mathrm{d}x = g\Delta\rho W(H-s). \tag{4}$$

Integration of equations (1) and (2) with the following boundary conditions:

$$\begin{aligned} y=0: &\quad u=0,\ T=T_w \\ y=\delta: &\quad u=0,\ T=T_f \end{aligned} \tag{5}$$

yields the solutions for the velocity and temperature

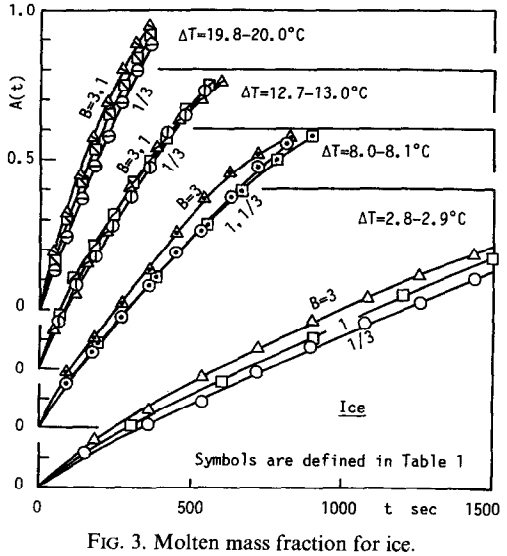

FIG. 3. Molten mass fraction for ice.

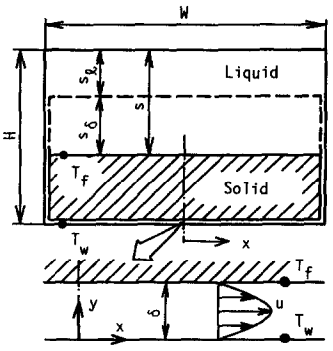

FIG. 4. Analytical model.

distributions in the liquid layer, respectively, as

$$u = \frac{1}{2\mu_l}\frac{\mathrm{d}p}{\mathrm{d}x}(y^2-\delta y) \tag{6}$$

$$T = T_w + (T_f - T_w)\frac{y}{\delta}. \tag{7}$$

Substitution of equations (6) and (7) into equation (3) yields

$$-\lambda_l(T_f-T_w)\int_0^x \frac{\mathrm{d}x}{\delta} = -\frac{\rho_l L}{12\mu_l}\frac{\mathrm{d}p}{\mathrm{d}x}\delta^3. \tag{8}$$

From the assumptions of equations (2) and (3), the liquid layer thickness, δ, is considered to be a constant with respect to x. Moallemi *et al.* [6] analyzed close-contact melting of rectangular solid on the assumption that (1) the energy transport by sensible heat in the liquid layer is not negligible as compared with that of latent heat, (2) the temperature distribution in the liquid layer is given by a parabolic function of y, and (3) the liquid layer thickness is given by an exponential series. They derived the result that δ is a constant for $Ste \ll 1$. Saito *et al.* [4] made a numerical analysis for close-contact melting of a cylindrical solid and found that δ can be considered to be a constant for $Ste < 0.159$.

The heat balance equation for $x = 0-x$ is given by neglecting the energy transport of sensible heat in the liquid layer as

$$-\lambda_l(T_f-T_w)\int_0^x \frac{\mathrm{d}x}{\delta} = \int_0^x mL \,\mathrm{d}x \tag{9}$$

where m (kg m^{-2} s^{-1}) is the molten mass fraction per unit area and unit time. When the solid melts keeping a level, m is constant for x and equation (9) can be integrated with respect to x. The thickness of the liquid layer is, then, given by integrating equation (9) to yield

$$\delta = \frac{\lambda_l(T_w-T_f)}{mL}. \tag{10}$$

Substitution of equation (10) into equation (8) and

integration with the boundary condition of $p = 0$ at $x = W/2$ yields

$$p = -6m^4\nu_l\left(\frac{C_{p_l}}{\lambda_l\, Ste}\right)^3\left[x^2-\left(\frac{W}{2}\right)^2\right]. \quad (11)$$

Substitution of equation (11) into equation (4) yields

$$m^4\nu_l\left[\frac{C_{p_l}W}{\lambda_l\, Ste}\right]^3 = g\Delta\rho W(H-s) \quad (12)$$

where m is given by

$$m = \rho_s\frac{ds_\delta}{dt}. \quad (13)$$

Dimensionless parameters are defined as

$$s^* = \frac{s}{W},\quad B = \frac{H}{W},\quad g^* = \frac{gW^3}{\nu_l^2},\quad \rho^* = \frac{\rho_l}{\rho_s}$$

$$\tau = Ste\, Fo,\quad A(\tau) = \frac{s}{H} = \frac{s^*}{B} \quad (14)$$

where $A(\tau)$ is a dimensionless molten mass fraction in the capsule. If it is assumed that the density change with melting is negligible ($\rho_l = \rho_s$) except for that in the buoyancy term, the molten mass fraction due to close-contact melting is given by substituting equation (13) into equation (12) to yield

$$\frac{d\tau}{ds_\delta^*} = \left(\frac{Ste}{g^*(1-\rho^*)Pr\, B}\right)^{1/4}\left(1-\frac{s^*}{B}\right)^{-1/4}. \quad (15)$$

Dimensionless representation of the liquid layer thickness is given by substituting equation (13) into equation (10) as $\delta/W = d\tau/ds_\delta^*$. The first term on the right-hand side in equation (15), which represents the ratio of degree of melting rate (Stefan number) to body force of the solid against the wall, is a dimensionless parameter governing the liquid layer thickness, δ^*

$$\delta^* = \frac{Ste}{g^*(1-\rho^*)Pr\, B}. \quad (16)$$

The dimensionless thickness of the liquid layer is derived from equations (15) and (16) as

$$\frac{\delta}{W} = \left[\frac{\delta^*}{1-A(\tau)}\right]^{1/4}. \quad (17)$$

On the other hand, the molten mass fraction due to heat conduction through the stable liquid at the top of the capsule is governed by the following equation on the assumption of a quasi-steady state condition:

$$\rho_s L\frac{ds_l}{dt} = \lambda_l\frac{(T_w-T_f)}{s}. \quad (18)$$

Dimensionless expression of equation (18) yields

$$\frac{ds_l^*}{d\tau} = \frac{1}{s^*}. \quad (19)$$

To obtain an approximate solution of equation (15), s^* ($=s_\delta^*+s_l^*$) is replaced by $s_\delta^*(1+C)$ where C is a constant value. Then, equation (15) can be integrated with the boundary condition of $A(\tau) = 0$ at $\tau = 0$ to yield

$$\tau = \tfrac{4}{3}\delta^{*1/4}B\{1-[1-A(\tau)]^{3/4}\}\frac{1}{1+C}. \quad (20)$$

Integration of equation (19) yields

$$\int ds_l^* = \frac{1}{B}\int\frac{d\tau}{A(\tau)}. \quad (21)$$

The value of C is given by

$$C = \frac{s_l^*}{BA(\tau)-s_l^*}. \quad (22)$$

The dimensionless molten mass fraction, $A(\tau)$, can be calculated by iteration of equations (20)–(22) as follows: at the time step of $\Delta\tau$, the value of $A(\tau)$ for $C = 0$ is calculated from equation (20); s_l^* is given from equation (21) by numerical integration; a new value of C is calculated from equation (22). The calculation is iterated until the value of C does not change and, thus, the analytical solution of $A(\tau)$ is obtained. The effect of time step on the solution was examined for $\Delta\tau = 0.005$, 0.01 and 0.02 and it was ascertained that $\Delta\tau = 0.005$ gives a satisfactorily precise solution.

Melting for ice

For the melting of ice, close-contact melting occurs at the top of the capsule, since the density of ice is smaller than that of water. The value of δ^* in equation (20) is, therefore, given by

$$\delta^* = \frac{Ste}{g^*(\rho^*-1)Pr\, B}. \quad (23)$$

At the bottom of the capsule, the liquid phase is stable for $T_w \leqslant 4°C$ and is unstable for $T_w > 4°C$ due to the density inversion of water at 4°C.

(a) For $T_w \leqslant 4°C$: the liquid phase is stable and, therefore, the same equations as (20)–(22) for the melting of octadecane are available.

(b) For $T_w > 4°C$: the liquid phase is unstable and natural convection occurs when the thickness of the liquid phase, s_l, exceeds a critical thickness, s_c. For $s_l < s_c$, the natural convection does not occur and therefore, equations (20)–(22) are available. For $s_l > s_c$, the following method is used.

For melting of the ice layer heated from below, Yen [7] examined the critical thickness, s_c, of the liquid phase for the natural convection to occur and also the heat transfer coefficient, h, of the natural convection which occurred

$$s_c = 152(T_w-T_f)^{-1.36} \quad (24)$$

$$h = 315\text{–}1900/(T_w-T_f) \quad (25)$$

where the range of application is for $7.7°C < T_w < 25.5°C$ and for 2.0 mm $< s_c <$ 10.2 mm. The heat balance equation at the solid–liquid interface is

given on the assumption of a quasi-steady state condition as

$$\rho_s L \frac{ds_l}{dt} = h(T_w - T_f). \quad (26)$$

Dimensionless expression of equation (26) yields

$$\frac{ds_l^*}{d\tau} = Nu_w \quad (27)$$

where $Nu_w = hW/\lambda_l$. Integration of equation (27) with the boundary condition of $s_l^* = s_c/W$ at $\tau = \tau_c$ yields

$$s_l^* = Nu_w(\tau - \tau_c) + \frac{s_c}{W} \quad (28)$$

where τ_c is a dimensionless time at the critical thickness, s_c. The solution for $\tau > \tau_c$ is obtained from equations (20), (22) and (28). It should be noted that substitution of both $\rho^* - 1 = \rho^*$ and $C = 0$ into equation (20) yields the same result as that of Moallemi *et al.* [6] which was derived for close-contact melting of rectangular solid for $Ste \ll 1$.

ANALYTICAL RESULTS AND DISCUSSIONS

Molten mass fraction

In Figs. 5 and 6, the analytical results of dimensionless molten mass fraction for octadecane and ice are compared with the experiments, respectively. For the aspect ratio of $B = 3$, it is seen that the experimental data show faster melting than the analytical results, because of the inclination of the solid to the side wall. For $B = 1/3$ and 1, some analytical results show slight difference from the experimental data. It is considered that the factors which cause the melting rate of the analytical results to be slower than the experiments are: in the analysis, (a) melting from the side walls was neglected, (b) the effect of natural convection between the side walls and the solid was neglected, and (c) the effect of melting from the side walls on pressure distribution in the liquid layer was neglected. On the contrary, the factors which cause the melting rate of the analytical results to be faster, are: in the experiment, (d) flow in the liquid layer was not asymptotic at $x = 0$, (e) a small amount of air bubbles in the solid accumulated into the liquid layer with melting, and (f) the condition of $Ste \ll 1$ was not satisfied. As a result, it is shown that the analytical results for $B = 1/3$ and 1 agree with the experimental data within the error of about 8% in $A(\tau)$.

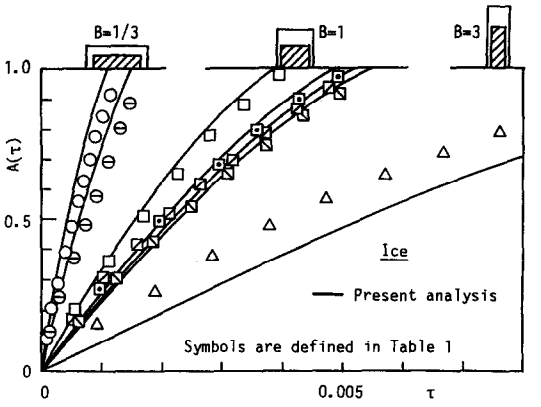

FIG. 6. Comparison between the analytical and experimental results for ice.

Liquid layer thickness

In Fig. 7, the variations of liquid layer thickness calculated from equation (17) are shown against the molten mass fraction. The results for both octadecane (solid lines) and ice (dashed lines) almost coincide with each other, because the difference between the δ^*s calculated from equations (16) and (23) is only 2% for the same value of Ste. For the melting outside a capsule, Saito *et al.* [5] reported that the liquid layer thickness was $\delta = 0.014$–0.16 mm for close-contact melting of the cylindrical solid. However, for the melting in a capsule, the thickness is large, about $\delta = 0.1$–0.4 mm as shown in Fig. 7. This is due to a weakness of body force of the solid in a capsule, where the motive force of the body force originates a density difference between the solid and the liquid. In Fig. 7, it is shown that δ increases more than 0.4 mm at the last stage of melting, which is caused by the decrease of body force with decreasing solid mass fraction. It is also shown that δ for $B = 1/3$ is larger than that for

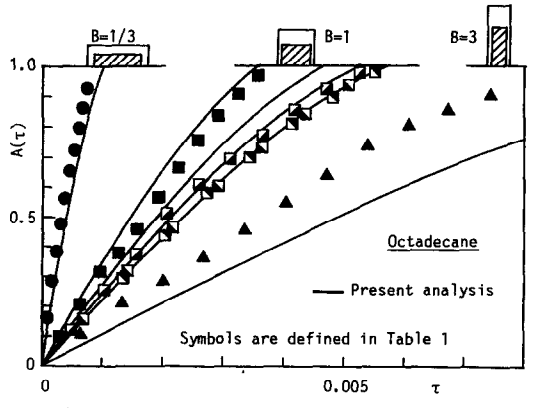

FIG. 5. Comparison between the analytical and experimental results for octadecane.

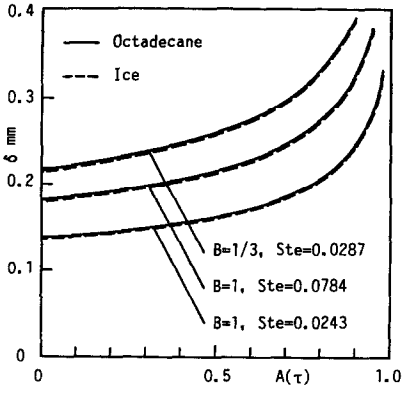

FIG. 7. Liquid layer thickness against molten mass fraction.

$B = 1$. Although the body forces for $B = 1/3$ and 1 are the same for the same solid volumes, the acting area for $B = 1/3$ is larger than that for $B = 1$.

From the above discussions, the value of δ in a capsule is comparatively large. Therefore, the range of Stefan number, in which the energy transport of sensible heat is negligible as compared with that of latent heat ($Ste \ll 1$), is considered to be different from that for the melting outside a capsule. The details on this point should be examined by, for example, numerical analysis and are a topic for the future.

Effects of heat conduction and natural convection in the liquid phase

In Fig. 8, the ratio of the molten mass fraction of the liquid phase (at the top of capsule for octadecane and at the bottom, for ice) to the total molten mass fraction is plotted against $A(\tau)$. For octadecane, the heat conduction through the liquid phase is dominant, since the liquid phase is stable. It is shown in Fig. 8 by the solid lines that the molten mass fraction by heat conduction is more than 10% of the total value at the early stage of melting, but it decreases to only about 2% at the last stage. On the other hand for ice, shown by the dashed lines, the natural convection occurs for $\Delta T(=T_w) > 4°C$. The effect for $\Delta T = 20.0°C$ is more than 10% during the melting. The tendency that this effect becomes larger at the last stage of melting is due to the decrease of melting rate by the close-contact, since the body force decreases with melting.

In Fig. 9, the ratios of the molten mass fraction of ice for $B = 1$ and $1/3$ are compared with each other. It is shown that the effect of natural convection is significantly larger for $B = 1/3$ as compared with that for $B = 1$. It implies that for larger aspect ratios, the effect of natural convection in the liquid phase cannot be neglected.

Dimensionless heat storage rate

Heat storage rate at a time τ per unit length of capsule is given by the sum of transferred heat rates

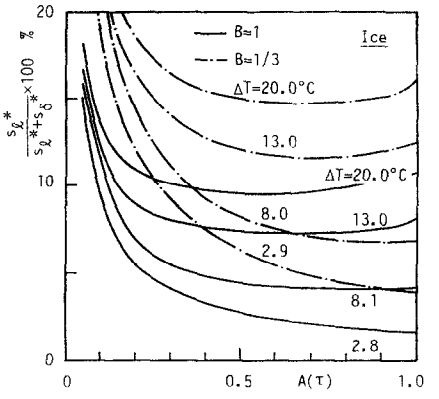

FIG. 9. Effects of heat conduction and natural convection in the liquid phase for ice.

from the top and bottom of the capsule

$$q = W\lambda_l \frac{T_w - T_f}{\delta} + \left[W\lambda_l \frac{T_w - T_f}{s} \quad \text{or} \quad Wh(T_w - T_f) \right]. \quad (29)$$

Neglecting the second and third terms on the right-hand side in equation (29) for the range of $Ste \ll 1$, and substituting equation (17) into equation (29), we have

$$q^* = \frac{q}{\lambda_l(T_w - T_f)} = \left[\frac{1 - A(\tau)}{\delta^*} \right]^{1/4}. \quad (30)$$

It is apparent from equation (30) that the dimensionless heat storage rate, q^*, is inversely proportional to $\delta^{*1/4}$. In Fig. 10, the qualitative tendency of q^* is compared with that for a cylindrical capsule by Bareiss and Beer [8], where their result is rearranged to be $q^*\delta^{*1/4} = 1$ at $A(\tau) = 0$. It is shown that for the melting in a cylindrical capsule, the heat storage rate decreases sharply with increasing molten mass fraction since the close-contact area decreases with melting. On the other hand, for a rectangular capsule, the close-contact area does not significantly change

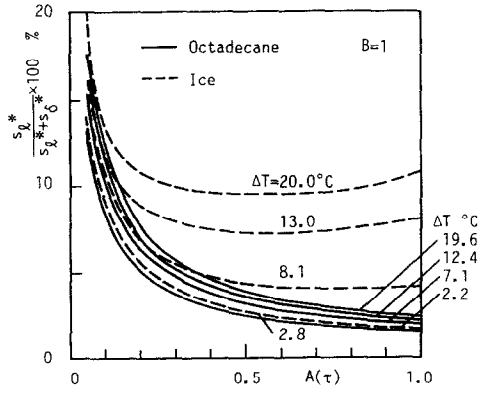

FIG. 8. Effects of heat conduction and natural convection in the liquid phase for $B = 1$.

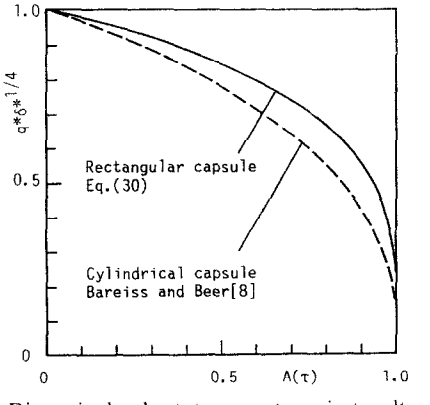

FIG. 10. Dimensionless heat storage rate against molten mass fraction.

and the heat storage rate is maintained at higher values than that for a cylindrical capsule. This implies that a rectangular capsule is appropriate to achieve constant rate of heat storage.

CONCLUSIONS

Experimental studies were performed for the close-contact melting in a rectangular capsule for octadecane and ice as PCM, respectively. The analysis applying Nusselt's liquid film theory to the heat transfer in the liquid layer was also made to examine the melting characteristics. The following conclusions may be drawn.

(1) There are two patterns of melting phenomena depending on aspect ratio of the capsule. One is that the melting occurs with keeping the solid at a level and the other, that the solid inclines to the side wall with melting. The melting rate for a square capsule ($B = 1$) is slower than that for other aspect ratios.

(2) The present simple method using Nusselt's liquid film theory is available to predict the melting rate in a rectangular capsule for $Ste \ll 1$.

(3) The liquid layer thickness for close-contact melting in a rectangular capsule is two to three times as large as that for outside the capsule.

(4) The effect of heat conduction through the liquid phase on total molten mass fraction is less than 2% and is negligible. However, the effect of natural convection is more than 10% for large Stefan numbers.

(5) To obtain constant rate of heat storage during melting, a rectangular capsule is more appropriate than a cylindrical one.

REFERENCES

1. A. Saito, T. Imamura, Y. Utaka and A. Saito, On the contact heat transfer with melting (4th Report), *Trans. JSME* **54,** 1123–1130 (1988), in Japanese.
2. S. Nagakubo and A. Saito, Numerical analysis on a direct contact melting process, *Trans. JAR* **4,** 37–45 (1987), in Japanese.
3. M. Okada, Characteristics of plate-fin heat exchanger with phase change material, *Trans. JAR* **5,** 125–132 (1988), in Japanese.
4. A. Saito, Y. Utaka, M. Akiyoshi and K. Katayama, Yooyu wo Tomonau Sesshoku Dennetsu no Kenkyu (2nd Report), *Trans. JSME* **50,** 2977–2984 (1984), in Japanese.
5. A. Saito, Y. Utaka and Y. Tokihiro, On contact heat transfer with melting (3rd Report), *Trans. JSME* **53,** 2130–2136 (1987), in Japanese.
6. M. K. Moallemi, B. W. Webb and R. Viskanta, An experimental and analytical study of close-contact melting, *J. Heat Transfer* **108,** 894–899 (1986).
7. Y. C. Yen, Free convection heat transfer characteristics in a melt water layer, *J. Heat Transfer* **102,** 550–556 (1980).
8. M. Bareiss and H. Beer, An analytical solution of the heat transfer process during melting of an unfixed solid phase change material inside a horizontal tube, *Int. J. Heat Mass Transfer* **27,** 739–746 (1984).

ANALYSE DE LA FUSION PAR CONTACT DE L'OCTADECANE ET DE LA GLACE DANS UNE CAPSULE RECTANGULAIRE HORIZONTALE CHAUFFEE A TEMPERATURE CONSTANTE

Résumé—Les caractéristiques de la fusion par contact de matériaux à changement de phase (PCM) dans des capsules rectangulaires horizontales sont examinées expérimentalement. Les capsules sont chauffées isothermiquement et on considère trois valeurs du rapport de forme ($H/W = 3$, 1 et 1/3). On utilise comme PCM respectivement l'octadécane et la glace. On présente une méthode d'analyse qui applique la théorie du film liquide de Nusselt au transfert de chaleur pendant la fusion par contact intime dans la capsule rectangulaire. Les résultats analytiques montrent un bon accord avec les données expérimentales. Pour la fusion de la glace, on trouve que l'effet de la convection naturelle résultant de l'inversion de densité de l'eau à 4°C devient significatif pour les grands nombres de Stefan.

UNTERSUCHUNGEN ÜBER DAS KONTAKTSCHMELZEN VON OKTADEKAN UND EIS IN ISOTHERM BEHEIZTEN RECHTECKIGEN EINSCHLÜSSEN

Zusammenfassung—Die Vorgänge beim Kontaktschmelzen eines Phasenwechselmaterials (PCM) innerhalb eines horizontalen, rechteckigen Einschlusses wird experimentell untersucht. Die Einschlüsse werden isotherm beheizt und stehen in drei verschiedenen Abmessungsverhältnissen ($H/W = 3$; 1 und 1/3) zur Verfügung. Oktadekan und Eis werden als PCM eingesetzt. Für die Untersuchung wird ein Verfahren benutzt, welches Nusselt's Filmtheorie auf das Kontaktschmelzen anwendet. Die Ergebnisse dieser Untersuchung zeigen eine gute Übereinstimmung mit Versuchswerten. Für das Schmelzen von Eis wird gezeigt, daß die natürliche Konvektion (bedingt durch die Dichteinversion von Wasser bei 4°C) bei großen Stefan-Zahlen von Bedeutung ist.

АНАЛИЗ ПЛАВЛЕНИЯ ОКТАДЕКАНА И ЛЬДА ПРИ ТЕСНОМ КОНТАКТЕ В ИЗОТЕРМИЧЕСКИ НАГРЕВАЕМОЙ ГОРИЗОНТАЛЬНОЙ ПРЯМОУГОЛЬНОЙ КАПСУЛЕ

Аннотация—Экспериментально исследуются характеристики плавления при тесном контакте исследуемых материалов, заключенных в горизоитальные прямоугольные капсулы. В экспериментах изотермически нагревались капсулы с тремя различными отношениями сторон (H/W = 3, 1 и 1/3). В качестве материалов с фазовым переходом использовались соответственно октадекан и лед. Анализ проводится с применением теории Нуссельта для жидкой пленки к теплопереносу при плавлении в условиях тесного контакта в прямоугольной капсуле. Результаты анализа хорошо согласуются с экспериментальными данными. В случае плавления льда найдено, что эффект естественной конвекции, обусловленный инверсией плотности воды при 4°C, становится существенным при больших числах Стефана.